Systematic error of microwave scatterometer wind related to the basin-scale plankton bloom

Hiroshi Hashizume[1] and W. Timothy Liu

Jet Propulsion Laboratory, California Institute of Technology, Pasadena, California, USA

Received 28 October 2003; accepted 13 February 2004; published 24 March 2004.

[1] Chlorophyll-a concentration derived from satellite ocean color sensor are compared with coincident wind speed difference between microwave scatterometer QuikSCAT product and reanalysis product from the National Center for Environmental Prediction over global oceans. The objective is to explore if a natural surface film, which originates in biological productivity, causes the underestimation of surface wind in scatterometer measurement by damping the small capillary wave through the surface tension. The wind speed difference (Reanalysis wind – QuikSCAT wind) is found to correlate positively with chlorophyll-a over the biologically highly productive areas, especially from intra-seasonal to seasonal time scales, indicating the surface film effect. The wind speed difference increases from ~ -1 m s^{-1} to ~ 0.5 m s^{-1} as chlorophyll-a increases from ~ 0.1 mg m^{-3} to ~ 3 mg m^{-3}, which is comparable with the results of previous laboratory experiments with artificial oil. *INDEX TERMS:* 4275 Oceanography: General: Remote sensing and electromagnetic processes (0689); 4506 Oceanography: Physical: Capillary waves; 4854 Oceanography: Biological and Chemical: Physicochemical properties; 4504 Oceanography: Physical: Air/sea interactions (0312); 4899 Oceanography: Biological and Chemical: General or miscellaneous. **Citation:** Hashizume, H., and W. T. Liu (2004), Systematic error of microwave scatterometer wind related to the basin-scale plankton bloom, *Geophys. Res. Lett.*, *31*, L06307, doi:10.1029/2003GL018941.

1. Introduction

[2] Microwave scatterometer has been developed mainly to measure the surface wind over the global ocean. A scatterometer sends microwave pulses to the surface and measures the backscattered power from surface roughness. Over the oceans, the surface roughness is caused by cm-scale capillary waves, which are believed to be in equilibrium of the surface wind stress. However, surface roughness is influenced not only by wind speed but also by secondary effects, such as sea surface temperature (SST) [e.g., *Liu*, 1984], atmospheric density stratification [e.g., *Liu*, 1984; *Wu*, 1991], surface current [e.g., *Kelly et al.*, 2001], rain [e.g., *Weissman et al.*, 2002], and surface film, all of which are neglected in the current standard wind retrieval algorithm. There is a large uncertainty about surface film effects because of the difficulty to obtain the surface film distribution. *Liu* [2002] gave a summary of the principles of scatterometry, the secondary effects on backscatter, and major scientific applications of scatterometer data.

[3] The ubiquitous surface film over the ocean originates from organic matter due to the biological productivity, and is thought to be one of the physically and chemically important factors in air-sea CO_2 exchange [*Frew et al.*, 1990; *Asher*, 1997; *Tsai and Liu*, 2003]. The surface film dampens the cm-scale capillary waves through the surface tension [*Alpers and Hühnerfuss*, 1989]. Therefore, the reduced backscatter due to the surface film's wave damping may cause underestimation in surface wind speed retrieval from scatterometers.

[4] Such backscatter reduction by the surface film has been long observed as 'slicks' by satellite Synthetic Aperture Radar (SAR) [e.g., *Clemente-Colon and Yan*, 1999; *Lin et al.*, 2002] and used for accidental oil spill detection. However, all of the previous studies have focused on the slicks in the small scale near the coastal region, taking advantage of the high resolution of SAR.

[5] The effects of surface film on scatterometer measurements have been found in the laboratory wind wave tank experiment (see *Alpers and Hühnerfuss* [1989] for reviews). There are also some airborne Ku-band scatterometer experiment studies [e.g., *Hühnerfuss et al.*, 1978; *Singh et al.*, 1986; *Gade et al.*, 1998]. There have been no observations of such effect on spacebased scatterometers in open ocean until the recent study by *Lin et al.* [2003]. They showed that backscatter reduction on QuikSCAT occurred near the chlorophyll-a-rich area in the northern North Atlantic. However, their study was limited to Sea-viewing Wide Field-of-View Sensor (SeaWiFS) images composited over just a few days.

[6] In this study, we attempt, for the first time, to describe the systematic error of the scatterometer wind caused by the natural surface film's wave damping effect, which is resulted from plankton blooming, over global oceans. Our emphasis is on the strong annual variation of biological productivity called spring bloom, which extends several thousand kilometers. The effect of natural surface film on scatterometer wind measurement in such large spatial scale and long time scale in the open ocean is important for climate study.

2. Data and Methodology

[7] Here, we make two assumptions; 1) Satellite-derived chlorophyll-a is used here as the alternative to the natural surface film since there are no global surface film dataset and it is known that phytoplankton can produce large amounts of natural surface film [*Zutic et al.*, 1981; *Frew et al.*, 1990; *Asher*, 1997]; 2) the wind speed difference between surface wind of global reanalysis and the scatterometer wind is used here as the scatterometer wind error

[1]Now at Department of Aerospace Engineering, Osaka Prefecture University, Sakai, Osaka, Japan.

0094-8276/04/2003GL018941$05.00

because 'true' surface winds are not sufficiently available in open oceans.

[8] Following the above assumption, we use space-borne ocean color sensor derived chlorophyll-a concentration (CHL) (mg m^{-3}) from SeaWiFS Level 3 data standard mapped image product. CHL is originally gridded at a 9 km × 9 km and daily resolution by NASA Goddard Space Flight Center, Earth Science Data Distribution Active Archive Center. For scatterometer wind measurement, we use the SeaWinds/QuikSCAT 10-m height equivalent neutral wind product (WQ) interpolated by a successive correction method [*Liu et al.*, 1998] to twice-daily 0.5° × 0.5° grid fields. We also use the 10-m height wind product of US National Centers for Environmental Prediction (NCEP)/National Center for Atmospheric Research (NCAR) Reanalysis [*Kalnay et al.*, 1996; *Kistler et al.*, 2001]. Since any scatterometer data have not been assimilated into the NCEP/NCAR reanalysis data, it is worth comparing them. To be consistent with QuikSCAT neutral wind product, the NCEP/NCAR 10-m height equivalent neutral wind (WN) is calculated from the 10-m height wind speed, air temperature and specific humidity at 2-m height, surface pressure, and SST of NCEP/NCAR reanalysis by using the surface-layer parameterization method of *Liu et al.* [1979].

[9] After re-gridding the above dataset from January 2000 to December 2001 onto 2.5° × 2.5° and 3-day average to be compared with each other, we define the wind speed difference as

$$dW = WN - WQ.$$

If the surface film is influential in the scatterometer wind causing the reduction of WQ, and the two assumptions mentioned above are valid, it is expected that dW increases (decreases) when CHL increases (decreases), that is, dW is positively correlated with CHL. In the following section, the local correlation between dW and CHL are globally examined and then, the time series of all variables and the dW dependency on CHL, WN and SST on each area where dW is positively correlated with CHL are shown.

3. Results

[10] The global distribution of biological productivity in the ocean is well observed by the space-borne ocean color sensor [e.g., *Yoder et al.*, 1993]. Three regions of high productivity and high correlation between dW and CHL are chosen for this study (Figure 1). The northern North Atlantic and the northern North Pacific are the most highly biologically productive regions except the coastal regions. In the southern Ocean, the highly biologically productive region is also seen as a band stretching eastward from the Cape Horn. In those areas, the biological productivity has a strong seasonality in the basin scale such as the rapid growth of phytoplankton in springtime. So-called 'spring bloom' is thought to be caused by the increase of the incident of sunlight in springtime with sufficient nutrients that have been brought near the surface by the mixing due to the strong wind in wintertime. As expected, most of the correlation coefficients over the highly biologically productive region are positive (Figure 1b), which is consistent with the expectation from the damping effect due to the natural surface film, except the coastal region. Biologically less-productive

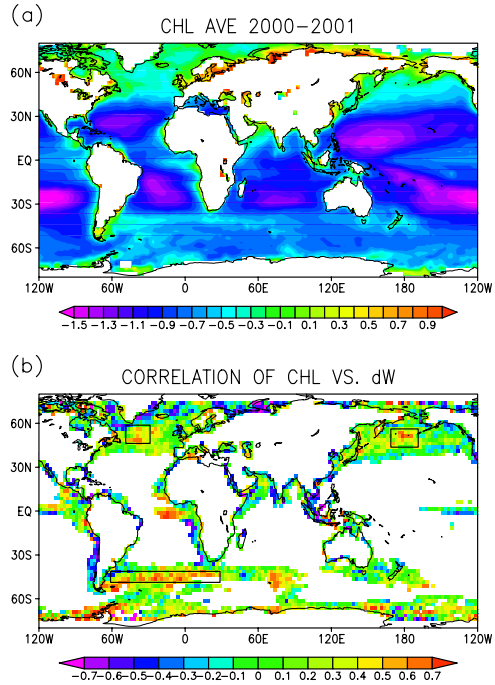

Figure 1. (a) SeaWiFS Chlorophyll-a concentration (CHL) (mg m^{-3}) averaged from 2000 to 2001. (b) Correlation coefficients of chlorophyll-a versus the wind difference (dW = NCEP/NCAR wind speed - QuikSCAT wind speed) (m s^{-1}). The calculation is avoided over biological less-productive region (logarithm of the averaged CHL < −0.7) (blank areas of the oceans) because the natural surface film is not expected to be important over such less-productive region. 30-day running average is applied to the data to pick up the seasonality. Three rectangles indicate the high correlation area that we focus on.

region ($\log_{10}$(CHL) < −0.7, see Figure 1a) is avoided in this study (blank areas of the oceans in Figure 1b) because the natural surface film is not expected to be important over such less-productive region. Although coastal regions are biologically productive in general, they are not examined in this study because of the uncertainty in the accuracy of nearshore scatterometer wind. The accuracy of scatterometer wind in the coastal region has been discussed by *Pickett et al.* [2003] and W. Tang et al. (Evaluation of high resolution ocean surface vector winds measured by QuikSCAT scatterometer in coastal region, submitted to *IEEE Transactions on Geoscience and Remote Sensing*, 2004). In spite of the relatively high positive correlation, the upwelling regions in the tropics are also avoided because the wind-induced upwelling is a dominant factor in the biological productivity, and the effects of CHL, SST, and wind speed on dW cannot be easily separated. For the above reasons, hereafter, we focus on the three regions in the sub-polar region, that is, the northern North Pacific, the northern North Atlantic, and the band in the Southern Ocean (three rectangles in Figure 1b).

[11] In Figure 2, dW are plotted against CHL in the three regions. The relations between dW and $\log_{10}$(CHL) are almost linear, and that dW increases from ∼−1 m s^{-1} to ∼0.5 m s^{-1} as CHL increases from ∼0.1 mg m^{-3} to ∼3 mg m^{-3}. This ∼1.5 m s^{-1} reduction of scatterometer wind is quantitatively reasonable relative to the previous

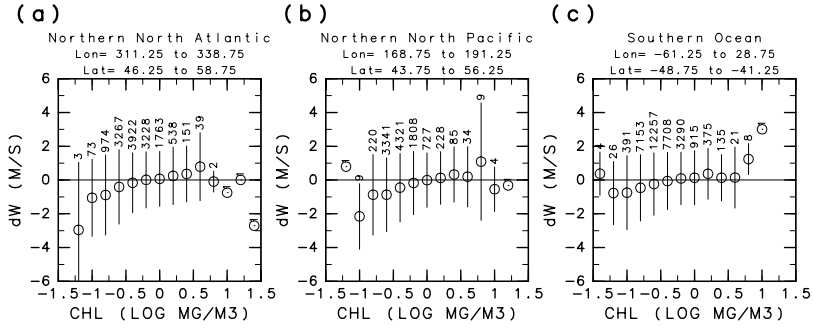

Figure 2. dW versus CHL in (a) the northern North Atlantic, (b) the northern North Pacific, and (c) the Southern Ocean. Each area is shown by a rectangle in Figure 1b. The average (circles), the plus and minus one standard deviation (error bars) and the number of data are calculated in bins of logarithm of CHL of 0.2.

experimental studies although it is much smaller than the amplitude of dW observed from instantaneous comparison by *Lin et al.* [2003]. For instance, *Feindt*'s [1985] laboratory wind wave tank experiments with X-band (9.8 GHz) scatterometer [see also *Alpers and Hühnerfuss*, 1989, Figure 5] shows that artificial surface film causes ∼7 dB backscatter reduction at 7 m s^{-1} wind speed, which corresponds to ∼3 m s^{-1} wind speed underestimation. *Singh et al.*'s [1986] field experiment with airborne scatterometer shows that the HH polarized backscatter depression in Ku-band (13.3 GHz) also increases from approximately 3–5 dB at 20° incident angle to ∼10 dB or more at 30°–40° incident angle and then decreases at the larger incidence angles. QuikSCAT is a Ku-band scatterometer with the incident angle 46° (horizontal polarization) and 54° (vertical polarization). That may be one of the reasons why the wind speed difference dependency on CHL in this study is smaller than the one of *Feindt*'s [1985] result.

[12] The large standard deviation (error bar) in Figure 2 may indicate that the dW dependency on CHL is affected by the other oceanic conditions such as SST as mentioned below. By limiting the range of SST (e.g., 284 < SST < 286 K), the standard deviation became somewhat smaller. However, the general features remain the same (not shown).

[13] There is no significant dW dependency on wind speed in the moderate condition, say 4 < WN < 10 m s^{-1} (not shown), which has been already shown in many previous comparisons between scatterometer and buoy wind [e.g., *Freilich and Dunbar*, 1999; *Quilfen et al.*, 2001; *Ebuchi et al.*, 2002].

[14] Attributing it to the water temperature-induced viscosity change, *Liu* [1984] has reported the Seasat scatterometer wind error dependency on SST under the weak wind condition (<6 m s^{-1}) using the ship-measured wind speed and SST. In this study, the dW dependence on SST is also examined area by area, but the dependency on SST is almost negligible relative to CHL and WN (not shown), which is consistent with *Ebuchi et al.*'s [2002] comparison between QuikSCAT and buoy wind.

[15] To visualize the correlation between CHL and dW in the seasonal timescale where CHL has basin-scale variation, time series of dW, CHL, SST, WN, and WQ are plotted area by area in Figure 3. Those time series are spatially averaged where the correlation coefficient between CHL and dW, r > 0.5 in each region (see Figure 1b). Generally, dW and CHL have almost no time delay (less than ∼3-day, which is temporal resolution of the data). This result is reasonable because surface film is expected to almost immediately affect the surface roughness and cause the scatterometer wind error. It is interesting that the well-known intraseasonal variation in CHL ('spring bloom' and 'fall bloom') seems to correspond to the one in dW in the northern North Pacific (vertical dashed lines in Figure 3b). On the other hand, SST has, generally, a couple of months time delay relative to CHL and dW, and no such double peaks as seen in CHL. WN also has no such clear double peaks although WN has a obvious seasonality. In addition to the many previous results that show no scatterometer wind dependency on wind speed under the moderate wind condition, the above results reinforce dW dependency on CHL, neither on SST nor WN.

4. Summary

[16] For the first time, satellite-derived SeaWiFS chlorophyll-a (CHL), QuikSCAT scatterometer wind speed (WQ), and NCEP/NCAR reanalysis surface wind speed (WN) and sea surface temperature (SST) are examined together over global oceans to describe the systematic error of the scatterometer wind related to plankton bloom.

[17] Focusing on the basin-scale high chlorophyll-a zone (the northern North Atlantic, the northern North Pacific, and the Southern Ocean), this study shows that dW and CHL are positively correlated with almost no time delay (less than 3 days). This tendency is consistent with the idea that natural surface film reduces the small cm-scale wave through the surface tension, causing the reduction of backscatter and the underestimation of scatterometer wind speed. The dW-CHL correlation in the subseasonal time scale gives further support to this effect. The dW dependency on $\log_{10}$(CHL) is almost linear, and dW increases from ∼−1 m s^{-1} to ∼0.5 m s^{-1} as CHL increases from ∼0.1 mg m^{-3} to ∼3 mg m^{-3}. This ∼1.5 m s^{-1} reduction of the scatterometer wind with the CHL increase is in quantitatively agreement with the results of the previous laboratory and field experiments with artificial surface film.

[18] The verification of the wind speed dependency on natural surface film might be important not only for microwave scatterometer but also microwave radiometer [*Alpers et al.*, 1982]. Comparing the Special Sensor Micro-

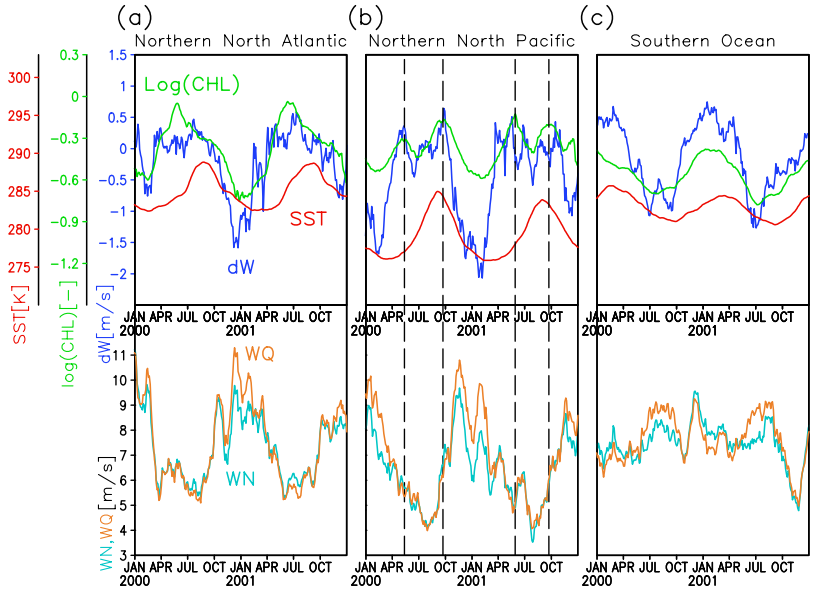

Figure 3. Time series of dW (m s^{-1}, dark blue), logarithm of CHL (mg m^{-3}, green), NCEP/NCAR SST (K, red), QuikSCAT wind speed (WQ) (m s^{-1}, orange), NCEP/NCAR wind speed (WN) (m s^{-1}, light blue) in (a) the northern North Atlantic, (b) the northern North Pacific, and (c) the Southern Ocean. Each time series is 30-day running-averaged and spatially-averaged where the correlation coefficient between dW and CHL is more than 0.5 in each area (rectangles in Figure 1b).

wave Imager (SSM/I) wind speed with the NCEP/NCAR wind speed, *Meissner et al.* [2001] show that the SSM/I wind's positive bias is significantly reduced in spring time over the sub-polar region, especially in the northern hemisphere [see *Meissner et al.*, 2001, Figures 4 and 5] although no clear reason for this has been shown. A part of them might be explained by natural surface film effect. We need more extensive field observations and the various satellite data analysis to confirm the results of this paper.

[19] **Acknowledgments.** The authors would like to thank Dr. W. Tang and Dr. S.-P. Xie for helpful discussions. This study was conducted at the Jet Propulsion Laboratory, California Institute of Technology, under contract with the National Aeronautics and Space Administration (NASA). The work has been supported by the Ocean Vector Winds Program of NASA.

References

Alpers, W., and H. Hühnerfuss (1989), The damping of ocean waves by surface films: A new look at an old problem, *J. Geophys. Res.*, *94*, 6251–6265.

Alpers, W., et al. (1982), The effect of monomolecular surface films on the microwave brightness temperature of the sea surface, *Int. J. Remote Sens.*, *3*, 457–474.

Asher, W. (1997), The sea surface microlayer and its effect on global air/sea gas transfer, in *The Sea Surface and Global Change*, edited by P. Liss and R. Duce, pp. 251–286, Cambridge Univ. Press, New York.

Clemente-Colon, P., and X.-H. Yan (1999), Observations of east coast upwelling conditions in synthetic aperture radar imagery, *IEEE Trans. Geosci. Remote Sens.*, *37*, 2239–2248.

Ebuchi, N., et al. (2002), Evaluation of wind vectors observed by QuikSCAT/SeaWinds using ocean buoy data, *J. Atmos. Oceanic Technol.*, *19, 2049–2062.*

Feindt, F. (1985), Radar-Rückstreuexperimente am Wind-Wellen-Kanal bei sauberer und filmbedeckter Wasseroberfläche im X-Band (9.8 GHz), *Hamb. Geophys. Einzelschr. Reihe Al 75*, 224 pp., Univ. Hamburg, Hamburg, Germany.

Freilich, M. H., and R. S. Dunbar (1999), The accuracy of the NSCAT 1 vector winds: Comparisons with National Data Buoy Center buoys, *J. Geophys. Res.*, *104*, 11,231–11,246.

Frew, N., et al. (1990), Impact of phytoplankton-generated surfactants on air-sea gas exchange, *J. Geophys. Res.*, *95*, 3337–3352.

Gade, M., et al. (1998), On the reduction of the radar backscatter by oceanic surface films: Scatterometer measurements and their theoretical interpretation, *Remote Sens. Environ.*, *66*, 52–70.

Hühnerfuss, H., et al. (1978), Measurements at 13.9 GHz of the radar backscattering cross section of the North Sea covered with an artificial surface film, *Radio Sci.*, *13*, 979–983.

Kalnay, E., et al. (1996), The NCEP/NCAR 40-year re-analysis project, *Bull. Am. Meteorol. Soc.*, *77*, 437–471.

Kelly, K. A., et al. (2001), Ocean currents evidence in satellite wind data, *Geophys. Res. Lett.*, *28*, 2469–2472.

Kistler, R., et al. (2001), The NCEP-NCAR 50-year reanalysis: Monthly means CD-ROM and documentation, *Bull. Am. Meteorol. Soc.*, *82*, 247–267.

Lin, I.-I., L.-S. Wen, K.-K. Liu, W.-T. Tsai, and A. K. Liu (2002), Evidence and quantification of the correlation between radar backscatter and ocean colour supported by simultaneously acquired in situ sea truth, *Geophys. Res. Lett.*, *29*(10), 1464, doi:10.1029/2001GL014039.

Lin, I.-I., W. Alpers, and W. T. Liu (2003), First evidence for the detection of natural surface films by the QuikSCAT scatterometer, *Geophys. Res. Lett.*, *30*(13), 1713, doi:10.1029/2003GL017415.

Liu, W. T. (1984), The effects of the variations in sea surface temperature and atmospheric stability in the estimation of average wind speed by SEASAT-SASS, *J. Phys. Oceanogr.*, *14*, 392–401.

Liu, W. T. (2002), Progress in scatterometer application, *J. Oceanogr.*, *58*, 121–136.

Liu, W. T., et al. (1979), Bulk parameterization of air-sea exchanges of heat and water vapor including the molecular constraints at the interface, *J. Atmos. Sci.*, *36*, 1722–1735.

Liu, W. T., et al. (1998), NASA scatterometer provides global ocean-surface wind fields with more structures than numerical weather prediction, *Geophys. Res. Lett.*, *25*, 761–764.

Meissner, T., et al. (2001), A 10 year intercomparison between collocated Special Sensor Microwave Imager oceanic surface wind speed retrievals and global analyses, *Geophys. Res. Lett.*, *106*, 11,731–11,742.

Pickett, M. H., et al. (2003), QuikSCAT satellite comparisons with nearshore buoy wind data off the U. S. west coast, *J. Atmos. Oceanic Technol.*, *20*, 1869–1879.

Quilfen, Y., et al. (2001), The ERS Scatterometer wind measurement accuracy: Evidence of seasonal and regional biases, *J. Atmos. Oceanic Technol.*, *18*, 1684–1697.

Singh, K. P., et al. (1986), The influence of surface oil on C- and Ku-band ocean backscatter, *IEEE Trans. Geosci. Remote Sens.*, *24*, 738–744.

Tsai, W.-T., and K.-K. Liu (2003), An assessment of the effect of sea surface surfactant on global atmosphere-ocean CO_2 flux, *J. Geophys. Res.*, *108*(C4), 3127, doi:10.1029/2000JC000740.

Weissman, D. E., et al. (2002), Effects of rain rate and wind magnitude on SeaWinds scatterometer wind speed errors, *J. Atmos. Oceanic Technol.*, *19*, 738–746.

Wu, J. (1991), Effects of atmospheric stability on ocean ripples: A comparison between optical and microwave measurements, *J. Geophys. Res.*, *96*, 7265–7269.

Yoder, J. A., et al. (1993), Annual cycles of phytoplankton chlorophyll concentrations in the global ocean: A satellite view, *Global Biogeochem. Cycles*, *7*, 181–193.

Zutic, V., et al. (1981), Surfactant production by marine phytoplankton, *Mar. Chem.*, *10*, 505–520.

H. Hashizume, Department of Aerospace Engineering, Osaka Prefecture University, 1-1 Gakuen-cho, Sakai-shi, Osaka-fu 599-8531, Japan. (zume@aero.osakafu-u.ac.jp)

W. T. Liu, Jet Propulsion Laboratory, California Institute of Technology, 4800 Oak Grove Drive, Pasadena, CA 91109-8099, USA.